



HAL
open science

Supramolecular Structure Characterization of Cellulose II Nanowhiskers Produced by Acid Hydrolysis of Cellulose I Substrates

Gilles Sèbe, Frédérique Ham-Pichavant, Emmanuel Ibarboure, Akissi Lydie
Chantal Koffi, Philippe Tingaut

► **To cite this version:**

Gilles Sèbe, Frédérique Ham-Pichavant, Emmanuel Ibarboure, Akissi Lydie Chantal Koffi, Philippe Tingaut. Supramolecular Structure Characterization of Cellulose II Nanowhiskers Produced by Acid Hydrolysis of Cellulose I Substrates. *Biomacromolecules*, 2012, 13 (2), pp.570-578. 10.1021/bm201777j . hal-00747623

HAL Id: hal-00747623

<https://hal.science/hal-00747623v1>

Submitted on 28 Sep 2024

HAL is a multi-disciplinary open access archive for the deposit and dissemination of scientific research documents, whether they are published or not. The documents may come from teaching and research institutions in France or abroad, or from public or private research centers.

L'archive ouverte pluridisciplinaire **HAL**, est destinée au dépôt et à la diffusion de documents scientifiques de niveau recherche, publiés ou non, émanant des établissements d'enseignement et de recherche français ou étrangers, des laboratoires publics ou privés.



Distributed under a Creative Commons Attribution - NonCommercial 4.0 International License

Supramolecular Structure Characterization of Cellulose II Nanowhiskers Produced by Acid Hydrolysis of Cellulose I Substrates

Gilles Sebe,^{*,†,‡} Frédérique Ham-Pichavant,^{†,‡} Emmanuel Ibarboure,^{†,‡} Akissi Lydie Chantal Koffi,[§] and Philippe Tingaut^{//}

[†] University of Bordeaux, LCPO, UMR 5629, F-33600 Pessac, France

[‡] CNRS, LCPO, UMR 5629, F-33600 Pessac, France

[§] Institut National Polytechnique Félix Houphouët-Boigny, LAPISEN, BP 1313 Yamoussoukro, Ivory Coast

^{//} Swiss Federal Laboratories for Materials Science and Technology (EMPA), CH-8600 Dübendorf, Switzerland

ABSTRACT: Cellulose II nanowhiskers (CNW-II) were produced by treatment of microcrystalline cellulose with sulfuric acid by both controlling the amount of H₂SO₄ introduced and the time of addition during the hydrolysis process. The crystalline structure was confirmed by both XRD and ¹³C CP-MAS NMR spectroscopy. When observed between crossed polarizers, the cellulose II suspension displayed flow birefringence and was stable for several months. The CNW-II nanowhiskers were significantly smaller than the cellulose I nanowhiskers (CNW-I) and had a rounded shape at the tip. The CNW-II average length and height were estimated by AFM to be 153 ± 66 and 4.2 ± 1.5 nm, respectively. An average width of 6.3 ± 1.7 nm was found by TEM, suggesting a ribbon-shape morphology for these whiskers. The average dimensions of the CNW-II elementary crystallites were estimated from the XRD data, using Scherrer's equation. A tentative cross-sectional geometry consistent with both XRD and NMR data was then proposed and compared with the geometry of the CNW-I nanowhiskers.

■ INTRODUCTION

In the current context of sustainability, there is a growing interest in developing novel polymer materials derived from renewable resources such as cellulose. In particular, recent research has shown that nanocellulose could be used to prepare a wide range of composite materials with improved properties.^{1–5} Cellulose in the plants is composed of 1,4- β -glucopyranose units associated by hydrogen bonding and forming a semicrystalline structure where highly ordered regions (the crystallites) are distributed among disordered domains (the amorphous phase). The molecular orientation and the hydrogen-bond network that tightly pack the cellulose chains within the crystallites can vary widely, giving rise to different polymorphs (cellulose I–IV), which structure depends on the cellulose source, method of extraction or treatment.^{3,6} With only a few exceptions, all native cellulose crystallites consist of cellulose I. They are nanometer-sized and can be recovered by various well-documented methods.^{1–5} Because of their high specific strength, modulus and aspect ratio, these nanocrystals, or cellulose nanowhiskers (CNW), can significantly improve the mechanical properties of polymers at low loading levels, and offer opportunities for new high value-added nanocomposite materials (films, adhesives, electronic devices, DNA-hybrid materials, foams, aerogels, and so on).^{1–5} Other advantages stem from their low density, renewable nature, abundance, biodegradability, and relatively low cost.

Among the different methods allowing the isolation of cellulose nanowhiskers from natural cellulose fibers, the most

employed has been to submit the initial cellulose substrate to concentrated sulfuric acid, combined with sonication. With this treatment, the amorphous regions of cellulose are hydrolyzed and rod-like cellulose nanowhiskers bearing anionic sulfate ester groups at their surface are produced. When they are dispersed in water, the cellulose nanowhiskers do not flocculate because of the electrostatic repulsions resulting from the negative surface charges, and the suspension is stable for several months.^{1–5} These suspensions have interesting characteristics since they are birefringent and can self-organize into stable chiral nematic phases when a critical concentration is reached (typical of liquid crystals).

Cellulose nanowhiskers can be prepared by acid hydrolysis of a wide variety of sources (tunicin, bacterial cellulose, wood, cotton, natural fibers, microcrystalline cellulose, and so on), their dimensions depending strongly on the initial material.^{2,5} The dimensions are also strongly impacted by the processing conditions i.e. sulfuric acid concentration, acid to fiber ratio, hydrolysis time, hydrolysis temperature, sonication time or ultrasonic irradiation intensity.^{7–10} But as far as the cellulose structure is concerned, the cellulose nanowhiskers generally retain their native cellulose I polymorph after hydrolysis of the amorphous domains.^{9–13}

Table 1. Conditions Used During the H₂SO₄ Addition for the Preparation of Various Types of Cellulose Nanowhiskers from MCC by Acidic Hydrolysis^a

sample No.	1	2	3	4	5	6	7	8	9
volume of H ₂ SO ₄ added (mL)	44	44	44	49	49	49	54	54	54
time of addition (min)	15	51	120	50	85	116	13	60	118
final appearance of the suspension	ivory white (i.w.)			translucent			i.w.	transparent	
final concentration in H ₂ SO ₄ (wt %)	62%			64%			66%		

^aConcentrated sulphuric acid was added to an initial dispersion of 10 g MCC in 50 mL of H₂O.

In the present work, we will show that cellulose II nanowhiskers can be produced by treatment of cellulose I substrates with sulfuric acid in certain conditions. Different types of cellulose nanowhiskers were prepared by adding dropwise various amounts of concentrated sulphuric acid to a water suspension of microcrystalline cellulose. The supra-molecular structure of the nanowhiskers was then characterized by X-ray diffraction (XRD), atomic force microscopy (AFM), transmission electron microscopy (TEM), and solid state ¹³C CP-MAS (cross-polarization–magic angle spinning) nuclear magnetic resonance (NMR).

EXPERIMENTAL SECTION

Materials. Cotton microcrystalline cellulose (powder) was purchased from Sigma Aldrich and sulphuric acid (95%) was purchased from Acros. Deionized water was used in all experiments.

Preparation of Cellulose Nanowhiskers. Cellulose nanowhiskers were prepared by adding dropwise various amounts of concentrated sulphuric acid to the initial microcrystalline cellulose (MCC) water dispersion, over various periods of time. A total of 10 g of MCC and 50 mL of water were placed in a beaker, and the suspension was stirred until a homogeneous dispersion was obtained. The beaker was immersed in an ice bath and 44, 49, or 54 mL of sulphuric acid (95 wt %) were added dropwise under stirring for 15–120 min. After the addition was complete, the suspension was heated at 44 °C for 30 min. The excess sulphuric acid was then removed by repeated centrifugation with deionized water (10 min, 4400 rpm) until the supernatant became turbid. The suspension was homogenized for 30 s with an Ultrathurax before each centrifugation. The turbid supernatant was then placed in a Spectra/Por dialysis membrane with a molecular weight cutoff of 3500 and dialyzed against water for 3 days, until the water pH remained constant. After the dialysis, the suspension was sonicated for 20 min, filtrated on a cellulose ester membrane (pores size = 5 μm), and freeze-dried.

¹³C CP-MAS NMR Spectroscopy. Solid state ¹³C CP-MAS NMR spectra of treated and unmodified samples were obtained at room temperature on a Bruker DPX-400 NMR spectrometer, using MAS rates of 4–8 kHz, at a frequency of 100.61 MHz. The freeze-dried cellulose nanowhiskers were packed in MAS 4 mm diameter zirconia rotors. Chemical shifts were relative to tetramethylsilane used as an external standard. All the spectra were run for 15 h (25000 scans).

X-ray Diffraction Analysis. X-ray diffraction (XRD) patterns were collected on a PANalytical X'pert MPD Bragg–Brentano θ – θ geometry diffractometer equipped with a secondary monochromator over an angular range of $2\theta = 8$ – 80° . The lyophilized cellulose nanowhiskers were put on sample holders made of aluminum alloy and flattened with a piece of glass. The Cu K α radiation was generated at 40 kV and 40 mA ($\lambda = 0.15418$ nm) and each acquisition was performed for 1 h 14 min.

The average dimensions L_{hkl} of the elementary crystallites perpendicular to the (1 $\bar{1}$ 0), (110), or (200) crystallographic plans was calculated according to the Scherrer's equation below, after measuring the full widths at half heights of the (hkl) diffraction peaks,

$$L_{hkl} = \frac{0.9 \lambda}{\beta_{1/2} \cos \theta}$$

where θ is the diffraction angle, λ is the wavelength of the X-ray radiation, and $\beta_{1/2}$ is the full width at half height of the diffraction peak.

Atomic Force Microscope (AFM). AFM measurements were performed at room temperature using a Veeco Dimension Icon AFM system equipped with a Nanoscope V controller. Both topographic and phase images of individual cellulose nanowhiskers were obtained in tapping mode using rectangular silicon cantilever (AC 160-TS, Atomic Force, Germany) with a spring constant of 42 N m⁻¹, a resonance frequency lying in the 290–320 kHz range, and a radius of curvature of less than 10 nm. The scan rates were in a range of 0.6 to 0.8 Hz. After dialysis, filtration, and sonication, the nanowhiskers suspensions were diluted to reach a 0.0014 wt % concentration. One droplet of 10–20 μL from dilute solutions was then deposited on a freshly cleaved mica surface and allowed to dry overnight at room temperature. Measurements of height, width, and spacing were taken using the section analysis tool provided with the AFM software (Nanoscope Analysis V1.20 from Bruker)

RESULTS AND DISCUSSION

Preparation of Cellulose II Nanowhiskers. Different types of cellulose nanowhiskers (CNW) were prepared by adding dropwise various amounts of concentrated sulphuric acid to the initial microcrystalline cellulose (MCC) water dispersion, over various periods of time. After the addition, all the dispersions were submitted to the same treatment (temperature, centrifugation, dialyse) according to a general procedure widely described in the literature.^{7–9} The different conditions used for the addition of H₂SO₄ in the MCC suspension are summarized in Table 1. The quality of the corresponding NWC dispersion obtained was evaluated by observing the mixture between cross-polarizers, the observation of flow-birefringence being used as a positive criterion for suspension stability.¹⁴ All the CNW suspensions were stable for several months and displayed flow birefringence when observed between crossed polarizers. After elimination of water from the different suspensions by freeze-drying, the CNW were analyzed by XRD, and the profiles obtained were reported in Figure 1. Depending on the addition conditions, different XRD patterns were obtained. Samples 1, 2, 3, and 7 show diffraction profiles characteristic of cellulose I, with peak maxima at 2θ angles of 15.1, 16.8, 21.0, 22.8, and 34.6° corresponding to the (1 $\bar{1}$ 0), (110), (012), (200), and (004) crystallographic planes, respectively.^{10,15–17} Additional diffraction peaks were observed at 11.6 and 31.8° in the profile of sample 7, but they could not be assigned at this stage of the study. The diffraction pattern of sample 8 on the other hand is typical of cellulose II, with the diffraction peaks at 12.2, 20.0, and 22.2° corresponding to the (1 $\bar{1}$ 0), (110), and (200) lattice planes.^{15,18,19} When observed between crossed polarizers, this cellulose II suspension displayed flow birefringence, indicating that the particles tend to self-organize into liquid crystalline arrangements like in the case of cellulose I nanowhiskers (Figure 2). The suspension was also stable for several months. To our knowledge, this is the first time that cellulose II nanowhiskers are directly produced

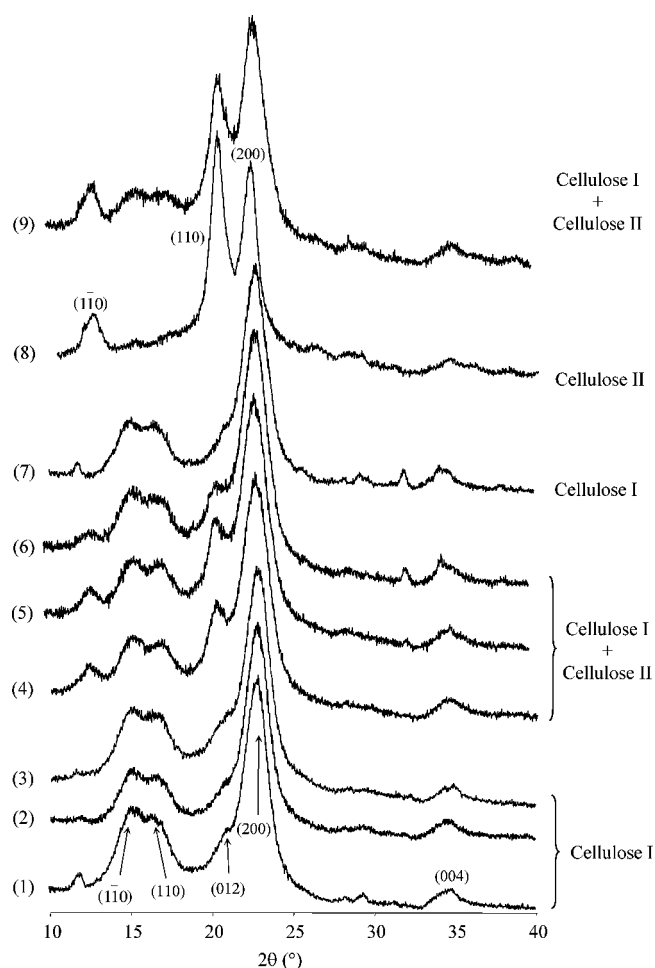


Figure 1. XRD profiles of the CNW prepared with the hydrolysis conditions reported in Table 1.

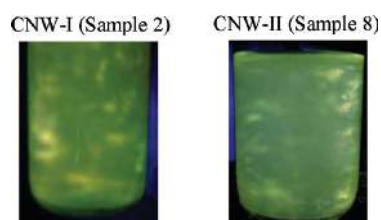


Figure 2. Aqueous 0.14 wt % suspensions of cellulose I (CNW-I) and cellulose II (CNW-II) nanowhiskers observed between cross-polarizers and showing flow birefringence.

from a cellulose I substrate during the H_2SO_4 hydrolysis process. A mixture of cellulose I and cellulose II was also produced in some cases, as indicated by the diffractions profiles of samples 4, 5, 6, and 9 in Figure 1. But at this stage of the study, it is difficult to state conclusively whether each particle is composed of a mixture of cellulose I and cellulose II polymorphs or whether a mixture of cellulose I particles and cellulose II particles is obtained. It should be noted that all the cellulose I dispersions displayed an ivory white appearance at the end of the H_2SO_4 addition, whereas the dispersions containing cellulose II were translucent or transparent (Table 1), indicating that the initial cellulose substrate was more degraded in that case.

Thus, by controlling both the amount of H_2SO_4 introduced and the time of addition during the hydrolysis step, cellulose II

nanowhiskers can be produced. A combination of long time of addition (>50 min) and high final acid concentration ($>64\%$ H_2SO_4) was necessary before any cellulose II structures could be observed (samples 4, 5, 6, 8, and 9). But pure cellulose II nanowhiskers were obtained only in a narrow range of conditions, that is, with 66% $\text{H}_2\text{SO}_4/60$ min addition (sample 8). The origin of this phenomenon has not been clearly identified at this stage of the study but the apparition of cellulose II nanocrystals could result from a mercerization effect under specific conditions (i.e., for a given H_2SO_4 concentration, time of contact, and temperature). Actually, it has been shown that treatments with concentrated mineral acids at room temperature can exert an effect upon cellulose, which is similar to that of strong aqueous alkali.²⁰ Accordingly, after an intermediate swelling with sulphuric acid and subsequent removal of the swelling agent at room temperature, the native cellulose I can be transformed into cellulose II.²¹ Another possibility would be that recrystallization of cellulose in the type II form occurred simultaneously with the chain splitting during the hydrolysis process, leading to the apparition of cellulose II nanocrystals.^{22–25} This recrystallization could be favored in the conditions of sample 8.

Microscopic Characterization. The AFM images of the cellulose I and cellulose II nanowhiskers (CNW-I and CNW-II, respectively) are compared in Figure 3. The CNW-I particles displayed the typical needle-like structure expected after partial acid hydrolysis of microcrystalline cellulose (or other cellulosic material), but the CNW-II nanowhiskers were significantly smaller and had a rounded shape at the tip. The distribution of particles length and thickness based on the topography images of Figure 3a,d are reported in Figure 4. The thickness was estimated from the height difference between the mica surface and the top of the nanocrystals. The width of the nanowhiskers was not accessible from the AFM scan because of broadening due to the convolution of the nanowhiskers and the AFM tip geometry.^{26,27} But the width is generally close to the height in the case of cellulose I nanowhiskers.²⁶ The CNW-II nanowhiskers tended to be shorter and thinner than the CNW-I ones, and their size distributions were less polydispersed. The average length and thickness were estimated (from Figure 4) to be 246 ± 128 and 5.9 ± 2.3 nm, respectively, for CNW-I and 153 ± 66 and 4.2 ± 1.5 nm, respectively, for CNW-II.

The TEM images of the CNW-II material confirmed the rod-like shape of the particles with the rounded tip (Figure 5) and allowed an estimation of the width, which was precluded by the AFM technique. An average width of 6.3 ± 1.7 nm was, accordingly, found for CNW-II, based on the particles width distribution in Figure 6. Therefore, by crossing the AFM and TEM results, a ribbon-shaped morphology can be proposed for the cellulose II nanowhiskers.

Investigation of the Crystallites Structure by XRD. The average dimensions L_{hkl} of the elementary crystallites perpendicular to the $(1\bar{1}0)$, (110) and (200) crystallographic planes of cellulose I and cellulose II whiskers can be calculated using the Scherrer's equation, by measuring the full widths at half heights of the different diffraction peaks, assuming that the finite size of crystallites dominate the broadening of the X-ray reflections.^{10,12,16,19,28} These values have to be considered as a lower bound since instrumental broadening and possible imperfections of the crystal lattice are neglected by the method. The results obtained from the XRD profiles of samples 1, 2, 3, 7, and 8 in Figure 1 are presented in Table 2. In the case of the CNW-I whiskers, only the length perpendicular to the (200)

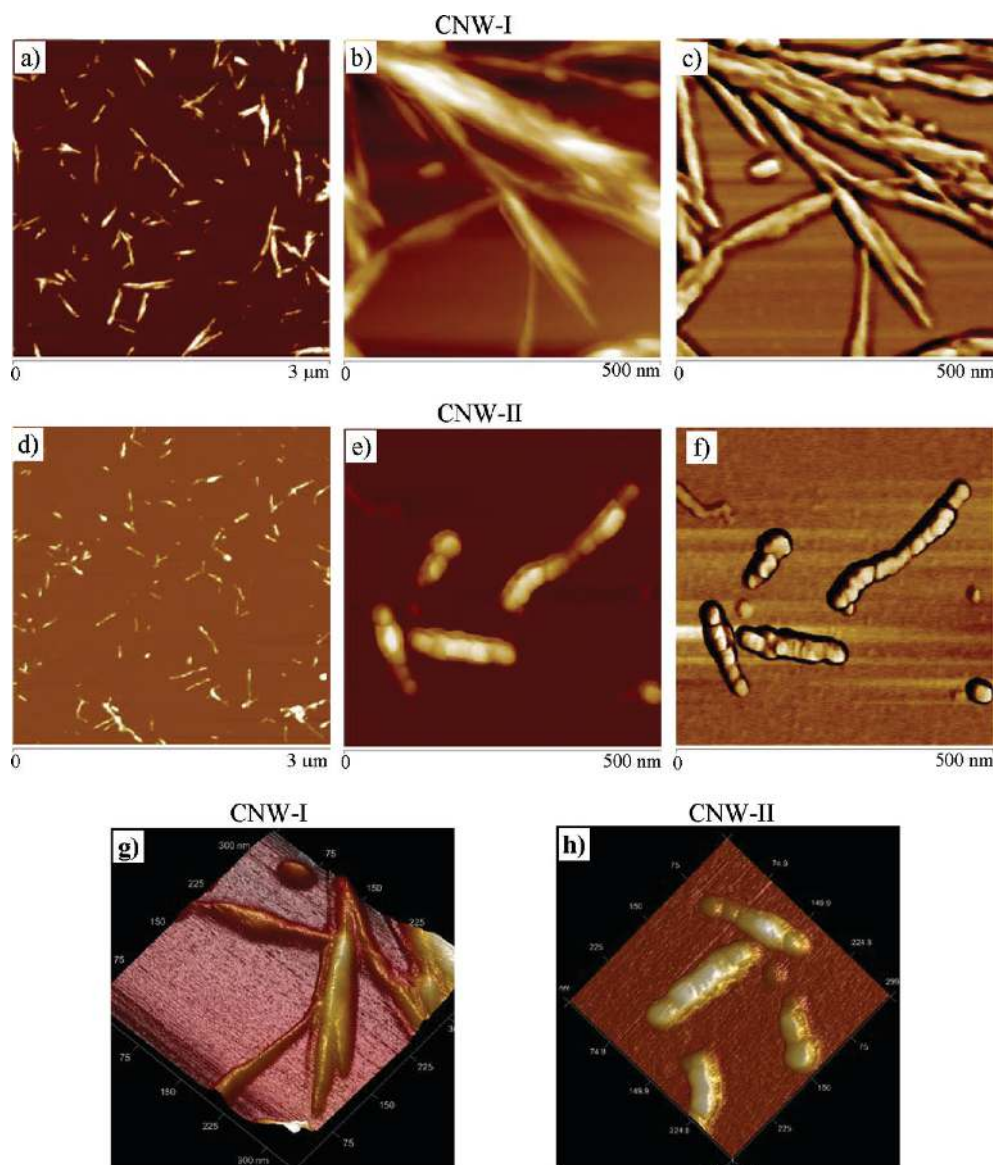


Figure 3. AFM images of the cellulose I and cellulose II nanowhiskers (CNW-I and CNW-II, respectively): topography images (a, b, d, e), phase images (c, f), and 3-D images (g, h).

plane could be calculated since the $(1\bar{1}0)$ and (110) reflections in the XRD profile overlapped. An average crystallite length of about 4.5 nm was obtained in that direction, which is consistent with reported values for microcrystalline cellulose.¹⁹ Larger crystallites were measured in the case of the CNW-II nanowhiskers, a value of about 6 nm being found along any of the three principal crystallographic directions of sample 8. It should be noted that these dimensions represent average values resulting from the XRD analysis of a macroscopic sample, but smaller elementary crystallites can be locally found in individual nanowhiskers, as confirmed by the CNW-II height profile of Figure 7 or the height measurements in Figure 4. The dimensions estimated by XRD were then combined and the cross-sectional geometry in Figure 8a was proposed to describe the average CNW-II elementary crystallite. The number of cellulose chains in each crystallographic plane was deduced from the XRD dimensions using the cellulose II d -spacings reported by Kolpak and Blackwell.²⁹ The CNW-II geometry obtained is consistent with results from Mukherjee and Woods,³⁰ which showed that, when forming a film by drying

a suspension of cellulose II nanocrystals (from mercerized cellulose), the $(1\bar{1}0)$ planes are parallel to the film surface. Thus, if this geometry is confirmed, the nanowhiskers in Figure 3 should stand on their $(1\bar{1}0)$ plane.

Concerning the CNW-I nanowhiskers, it is generally assumed that their elementary crystallites have a square cross-section, which lateral dimensions vary depending on the plant source.^{10,31} Accordingly, the CNW-I cross-sectional geometry in Figure 8b can be proposed, based on the XRD dimension measured in the (200) direction, and on the d -spacings reported by Sugiyama et al.³² With this geometry, the CNW-I nanowhiskers in Figure 3 can stand either on the $(1\bar{1}0)$ plane or the (110) plane.

Investigation of the Crystallites Structure by ^{13}C CP-MAS NMR. The CNW-I and CNW-II nanowhiskers were further characterized by ^{13}C CP-MAS NMR spectroscopy (Figure 9). The different resonances observed in the NMR spectra correspond to different conformations for the anhydroglucose units.^{31,33–35} The NMR spectra of CNW-I and CNW-II are characteristic of cellulose I and cellulose II

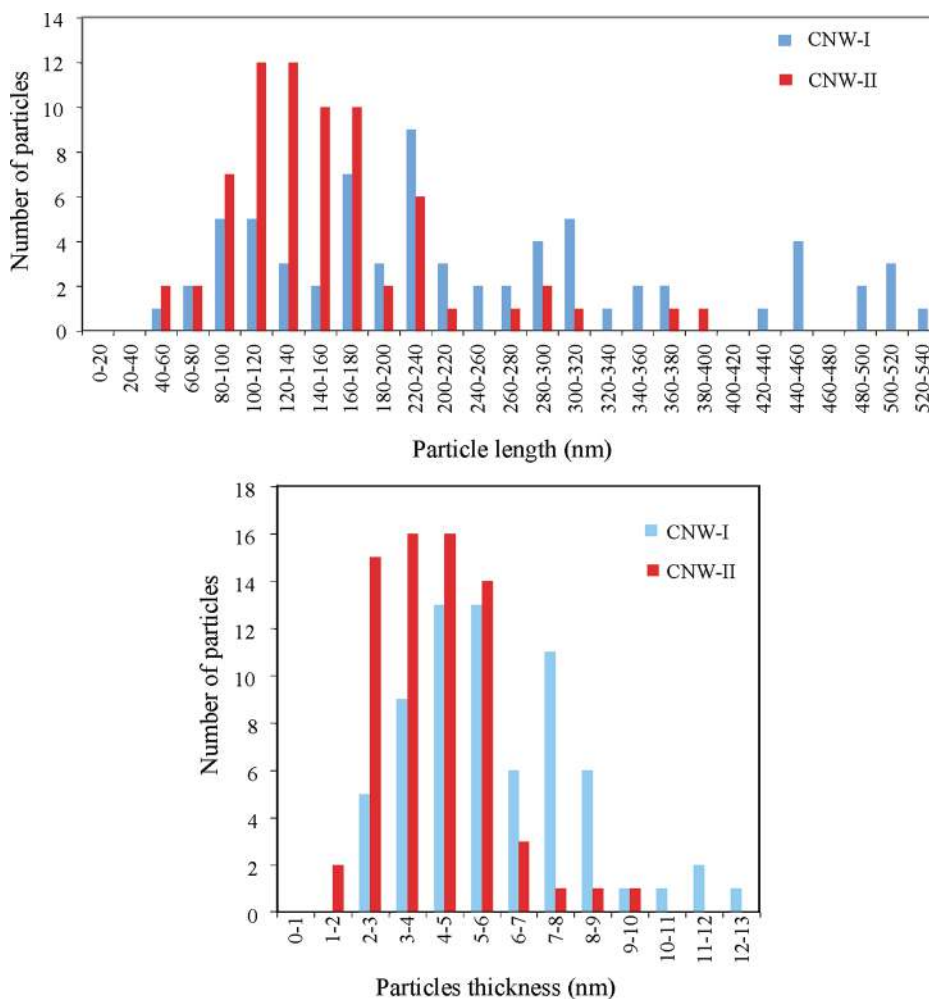


Figure 4. Distribution of particles length and thickness of cellulose I (CNW-I) and cellulose II (CNW-II) nanowhiskers, estimated from the AFM images.

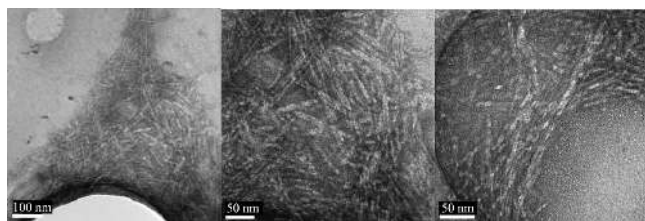


Figure 5. TEM images of the cellulose II nanowhiskers (CNW-II).

crystalline polymorphs, respectively,^{15,18,31,35–38} confirming the XRD results. The region between 60 and 70 ppm is assigned to C_6 of the primary alcohol group. The next cluster between 70 and 80 ppm is attributed to the C_2 , C_3 , and C_5 carbons. The region between 80 and 95 ppm is associated with C_4 and that between 100 and 110 ppm with the anomeric carbon C_1 . The NMR spectrum of CNW-I differs from that of CNW-II in these regions because of differences in the chain conformations of the cellulose I and cellulose II polymorphs.^{18,36,37} The small peak at about 96 ppm in the CNW-II spectrum has been assigned to C_1 carbons of the end monomer units, which can be distinguished when the degree of polymerization of cellulose is sufficiently low.^{34,37} Hence, the CNW-II cellulose chains are apparently shorter than the CNW-I chains.

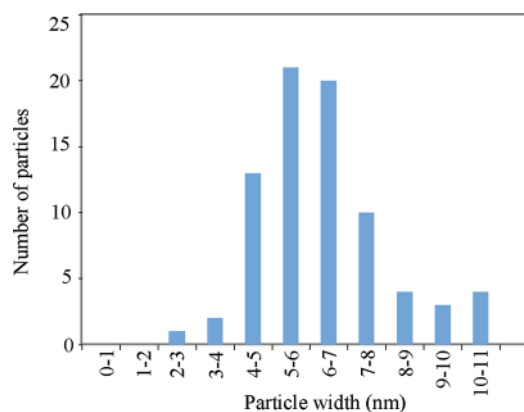


Figure 6. Distribution of particles width of the cellulose II nanowhiskers (CNW-II) estimated from the TEM images.

From the NMR spectra, it is also possible to evaluate the lateral dimensions of the whiskers elementary crystallites, by comparing the contributions from chains buried within the crystallites and chains exposed at the surface of the nanowhiskers in the C_4 region.³¹ In the CNW-I spectrum, the narrower signal at 89 ppm corresponds to anhydroglucose units in a highly ordered environment, that is, in the interior of the crystallites. The broader one at 84 ppm corresponds to a more

Table 2. Average Dimension L_{hkl} of the CNW-I and CNW-II Elementary Crystallites Perpendicular to the Direction of the $(1\bar{1}0)$, (110) , or (200) Crystallographic Planes Estimated by XRD

sample No.	cellulose polymorph	L (nm)		
		$L_{1\bar{1}0}$	L_{110}	L_{200}
1	I			4.5
2	I			4.8
3	I			4.3
7	I			4.5
8	II	6.0	6.4	6.0

diverse distribution of structural arrangements (i.e., a lower degree of order) and is characteristic of the anhydroglucoses at the surface.^{31,33,34} The contributions from chains buried within the crystallites and chains exposed at the surface are then obtained from the integration of the C_4 signals of interior and surface chains at 89 and 84 ppm, respectively (Figure 10). The fraction of interior chains is estimated from the NMR signal by calculating a parameter X defined by $X = (\text{area between } 86.2 \text{ and } 93.9 \text{ ppm}) / (\text{area between } 80.3 \text{ and } 93.9 \text{ ppm})$. Assuming a square cross-section, the cellulose I crystallites can be approximated by an array of $n \times n$ cellulose chains with a lattice angle of 90° and average d -spacing of $h = 0.57$ nm (Figure 10).³¹ With this geometry, the fraction of cellulose chains contained in the interiors of crystallites (i.e., the X parameter) is estimated by the ratio of the area in blue (Figure 10) to the total area of the cross-section. Hence, the X parameter is related to the lateral dimensions of the crystallites L by the relation $X = (L - 2h)^2 / L^2$, which can be rearranged to $L = 2h / (1 - X^{1/2})$. This method has been shown to be particularly reliable to assess the size of cellulose I crystallites with relatively narrow lateral dimensions.³¹ Dimensions of about 5 nm were found for CNW-I, in the directions perpendicular to the $(1\bar{1}0)$ and (110) planes, which is about 1 nm more than our estimation by XRD in Figure 8b. But the dimensions of the whiskers could be underestimated by the XRD method, because instrumental broadening and possible imperfections of the crystal lattice are neglected by the method. It is also possible that, due to weaker intersheet interactions between the (200) plans, some delamination occurred during the exhaustive acid hydrolysis process, as was recently reported.¹² In that case, the CNW-I elementary crystallites would have the cross-sectional geometry proposed in Figure 11a. With this geometry, the fraction of cellulose chains contained in the interior of crystallites can be estimated from Figure 10b by the ratio of the area in blue to the total area of the cross-section. Hence, by decomposing the elementary crystallite into triangular subunits, the fraction of cellulose

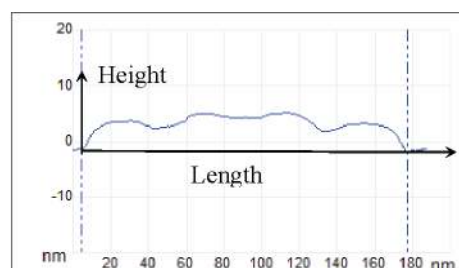
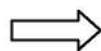
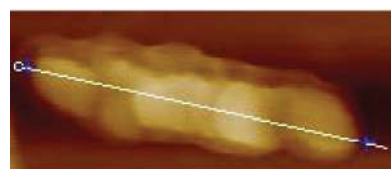


Figure 7. AFM topography image and height profile of a typical CNW-II nanowhisker.

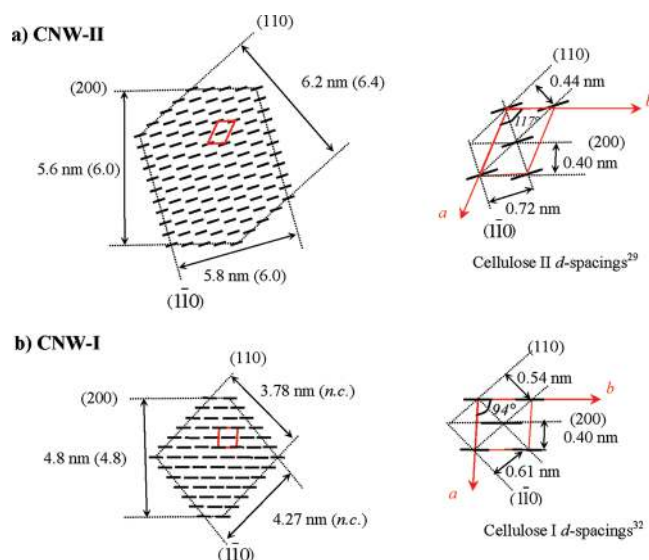


Figure 8. Cross sections of CNW-II (a) and CNW-I elementary crystallites (b) deduced from the XRD profiles. The short bars indicate the projection of cellulose molecules. The dimensions estimated from the d -spacings and from the XRD data (in brackets) are reported. The cellulose II and cellulose I monoclinic unit cells (in red) and the principal lattice planes are also reported; n.c. = noncalculated.

chains contained in the interiors of crystallites can be estimated by $X = (\text{number of interior triangular subunits}) / (\text{total number of triangular subunits})$. The value obtained ($X = 0.62$) is closed to the value measured by NMR ($X = 0.61$), so this geometry would be consistent with both NMR and XRD results.

Using the same approach, we tentatively tried to verify if the geometry proposed in Figure 8a for CNW-II, was also consistent with the NMR data. It has been reported that crystalline cellulose II resonates as a doublet at 88 and 89 ppm, whereas the surface signal is expected between 82 and 87 ppm (Figure 12a).³⁹ The fraction of cellulose chains contained in the interiors of the cellulose II crystallites can accordingly be estimated from the C_4 region of the NMR spectrum by $X = (\text{area between } 86.7 \text{ and } 94.2 \text{ ppm}) / (\text{area between } 80.3 \text{ and } 94.2 \text{ ppm})$. The value obtained ($X = 0.69$) is rather consistent with the value estimated from the geometry proposed in Figure 8a ($X = 0.66$; see calculation in Figure 12b). However, the signal overlapping between the interior and surface chains in the C_4 region of the NMR spectrum is more important for CNW-II than for CNW-I. Therefore, the X parameter calculated by NMR for CNW-II is certainly approximative.

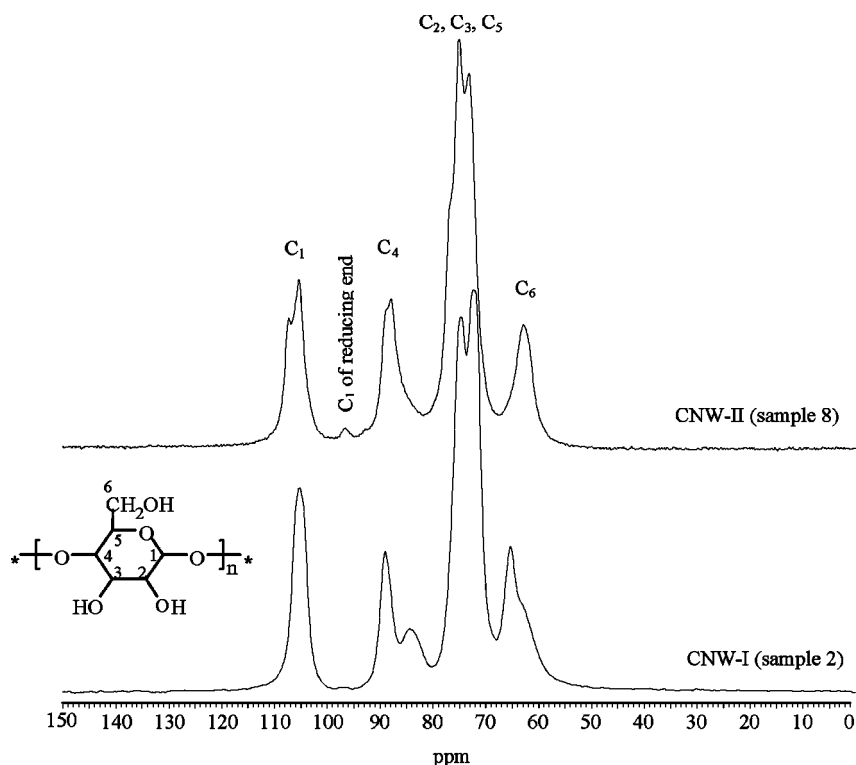


Figure 9. ^{13}C CP-MAS NMR spectra of CNW-I and CNW-II nanowhiskers with the corresponding chemical shifts assignments.

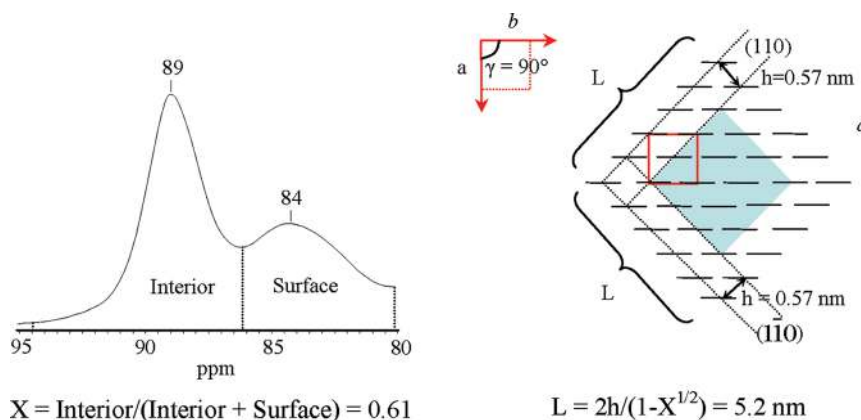


Figure 10. Evaluation of the CNW-I crystallites dimensions by ^{13}C CP-MAS NMR spectroscopy according to the method of Newman.³¹ The short bars indicate the projection of cellulose molecules. A 6×6 array of 36 cellulose chains is represented as an example.

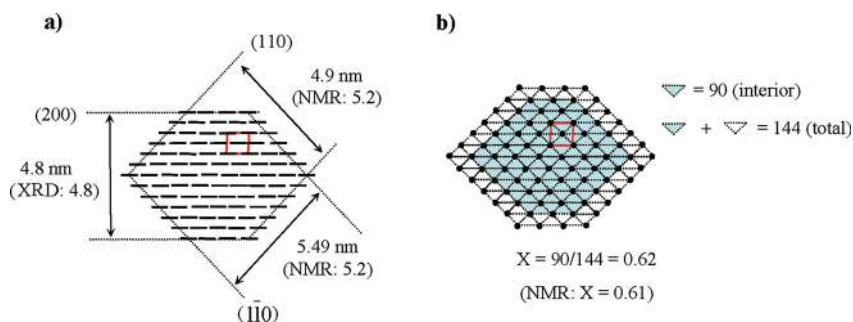


Figure 11. Tentative representation of the cross sections of CNW-I elementary crystallites consistent with both NMR and XRD data. The dimensions estimated from the d -spacings (Sugiyama et al., 1991) and from the XRD or NMR data (in brackets) are reported on the left scheme (a). The right scheme (b) was used to estimate the X parameter from the proposed geometry and verify its consistency with the NMR data. The short bars or dots indicate the projection of cellulose molecules. The cellulose I monoclinic unit cell (in red) is also reported.

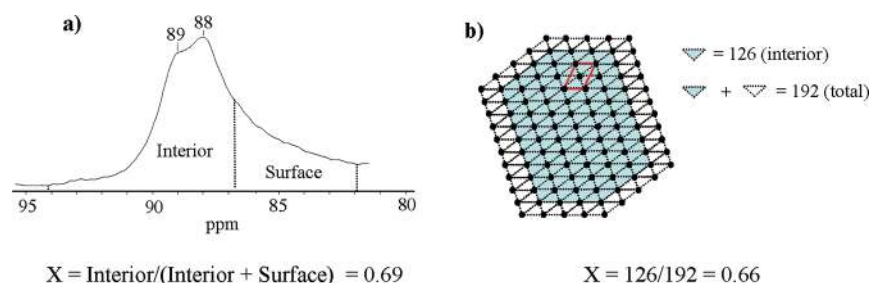


Figure 12. Comparison of the X parameters for CNW-II, calculated from the NMR spectrum (a) or from the cross-sectional geometry suggested by the XRD data in Figure 8a (b). The dots indicate the projection of cellulose molecules. The cellulose II monoclinic unit cell (in red) is also reported.

CONCLUSIONS

In conclusion, we have found that the treatment of microcrystalline cellulose with sulfuric acid could produce cellulose II nanowhiskers (CNW-II), within a narrow range of conditions controlled by the amount of H_2SO_4 introduced and the time of addition. To our knowledge, this is the first time that cellulose II nanowhiskers are directly produced from a cellulose I substrate during the H_2SO_4 hydrolysis process. The CNW-II aqueous suspension was stable for several months and displayed flow birefringence when observed between crossed polarizers, like in the case of cellulose I nanowhiskers (CNW-I). But the morphology of the CNW-II particles differed significantly from that of the needle-shaped CNW-I: the cellulose II nanowhiskers were smaller and displayed a ribbon-shaped morphology with rounded tips. According to calculations based on the XRD and NMR data, the average dimensions and geometry of the CNW-II elementary crystallites were also very different. The CNW-II crystallites were estimated to be larger than the CNW-I ones, and the cellulose chains within the crystallites were oriented differently. Hence, the controlled hydrolysis of cellulose substrates by H_2SO_4 could provide a facile approach to prepare a new generation of cellulose nanowhiskers with an increased surface area and original supramolecular structure, which could find application in the area of nanocomposites. The ribbon-shaped morphology of the CNW-II particles for instance, could have a positive impact on the barrier properties of nanocomposite films reinforced with these whiskers. Potential applications in optoelectronics are also anticipated.

AUTHOR INFORMATION

Corresponding Author

*E-mail: gilles.sebe@u-bordeaux1.fr.

Notes

The authors declare no competing financial interest.

ACKNOWLEDGMENTS

The authors are grateful to Eric Lebraud for running the XRD experiments.

REFERENCES

- (1) Eichhorn, S. J.; Dufresne, A.; Aranguren, M.; Marcovich, N. E.; Capadona, J. R.; Rowan, S. J.; Weder, C.; Thielemans, W.; Roman, M.; Renneckar, S.; Gindl, W.; Veigel, S.; Keckes, J.; Yano, H.; Abe, K.; Nogi, M.; Nakagaito, A.; Mangala, A.; Simonsen, J.; Benigh, A. S.; Bismark, A.; Berglund, L. A.; Peijs, T. *J. Mater. Sci.* **2010**, *45*, 1–33.
- (2) Siqueira, G.; Bras, J.; Dufresne, A. *Polymers* **2010**, *2*, 728–765.
- (3) Habibi, Y.; Lucia, L. A.; Rojas, O. J. *Chem. Rev.* **2010**, *110*, 3479–3500.

- (4) Klemm, D.; Kramer, F.; Moritz, S.; Lindström, T.; Ankerfors, M.; Gray, D.; Forris, A. *Angew. Chem., Int. Ed.* **2011**, *50*, 5438–5466.
- (5) Eichhorn, S. J. *Soft Matter* **2011**, *7*, 303–315.
- (6) O'Sullivan, A. C. *Cellulose* **1997**, *4*, 173–207.
- (7) Dong, X. M.; Revol, J.-F.; Gray, D. G. *Cellulose* **1998**, *5*, 19–32.
- (8) Beck-Candanedo, S.; Roman, M.; Gray, G. *Biomacromolecules* **2005**, *6*, 1048–1054.
- (9) Bondeson, D.; Mathew, Aji; Oksman, K. *Cellulose* **2006**, *13*, 171–180.
- (10) Elazzouzi-Hafraoui, S.; Nishiyama, Y.; Putaux, J.-L.; Heux, L.; Dubreuil, F.; Rochas, C. *Biomacromolecules* **2008**, *9*, 57–65.
- (11) Lu, P.; Hsieh, Y.-L. *Carbohydr. Polym.* **2010**, *82*, 329–336.
- (12) Li, Q.; Renneckar, S. *Biomacromolecules* **2011**, *12* (3), 650–659.
- (13) Çetin, N. S.; Tingaut, P.; Özmen, N.; Henry, N.; Harper, D.; Dadmun, D.; Sèbe, G. *Macromol. Biosci.* **2009**, *9*, 997–1003.
- (14) Azizi Samir, M. A. S.; Alloin, F.; Sanchez, J.-Y.; El Kissi, N.; Dufresne, A. *Macromolecules* **2004**, *37*, 1386–1393.
- (15) Isogai, A.; Usuda, M.; Kato, T.; Uryu, T.; Atalla, R. H. *Macromolecules* **1989**, *22*, 3168–3172.
- (16) Garvey, C. J.; Parker, I. H.; Simon, G. P. *Macromol. Chem. Phys.* **2005**, *206*, 1568–1575.
- (17) Heath, L.; Thielemans, W. *Green Chem.* **2010**, *12*, 1148–453.
- (18) Takahashi, M.; Takenaka, H. *Polym. J.* **1987**, *19*, 855–861.
- (19) Wada, M.; Ike, M.; Tokuyasu, K. *Polym. Degrad. Stab.* **2010**, *95*, 543–548.
- (20) Heuzer, T. *the Chemistry of Cellulose*; John Wiley and Sons: New York, 1944; pp 133–135.
- (21) Rånby, B. G. *Acta Chem. Scand.* **1952**, *6*, 101–115.
- (22) Hermans, P. H.; Weidinger, A. J. *Polym. Sci.* **1949**, *IV*, 317–322.
- (23) Battista, O. A. *Ind. Eng. Chem.* **1950**, *42*, 502–507.
- (24) Tang, L.-G.; Hon, D. N.-S.; Pan, S.-H.; Zhu, Y.-Q.; Wang, Z.; Wang, Z.-Z. *J. Appl. Polym. Sci.* **1996**, *59*, 483–488.
- (25) Ibbett, R. N.; Domvoglou, D.; Philips, D. A. S. *Cellulose* **2008**, *15*, 241–254.
- (26) Kvien, I.; Tanem, B. S.; Oksman, K. *Biomacromolecules* **2005**, *6*, 3160–3165.
- (27) Cao, X.; Dong, H.; Li, C. M. *Biomacromolecules* **2007**, *8*, 899–904.
- (28) Jakob, H. F.; Fengel, D.; Tschegg, S. E.; Fratzl. *Macromolecules* **1995**, *28*, 8782–8787.
- (29) Kopak, F. J.; Blackwell, J. *Macromolecules* **1976**, *9*, 273–278.
- (30) Mukherjee, S. M.; Woods, H. J. *Biochim. Biophys. Acta* **1953**, *10*, 499–511.
- (31) Newman, R. H. *Solid State Nucl. Magn. Reson.* **1999**, *15*, 21–29.
- (32) Sugiyama, J.; Vuong, R.; Chanzy, H. *Macromolecules* **1991**, *24*, 4168–4175.
- (33) Earl, W. L.; VanderHart, D. L. *Macromolecules* **1981**, *14*, 570–574.
- (34) Maciel, G. E.; Kolodziejski, W. L.; Bertran, M. S.; Dale, B. E. *Macromolecules* **1982**, *15*, 686–687.
- (35) Atalla, R. H.; VanderHart, D. L. *Solid State Nucl. Magn. Reson.* **1999**, *15*, 1–19.
- (36) Atalla, R. H.; Gast, J. C.; Sindorf, D. W.; Bartuska, G. E.; Maciel, G. E. *J. Am. Chem. Soc.* **1980**, *102*, 3249–3251.

(37) Dudley, R. L.; Fyfe, C. A.; Stephenson, P. J.; Deslandes, Y.; Hamer, G. K.; Marchessault, R. H. *J. Am. Chem. Soc.* **1983**, *105*, 2469–2472.

(38) Viëtor, R. J.; Newman, R. H.; Ha, M. A.; Apperley, D. C.; Jarvis, M. C. *Plant J.* **2002**, *30*, 721–731.

(39) Ibbett, R. N.; Domvoglou, D.; Fasching, M. *Polymer* **2007**, *48*, 1287–1296.